Effect of a Transmission Line Resonator on a Small Capacitance Tunnel Junction

T. Holst,* D. Esteve, C. Urbina, and M. H. Devoret
Service de Physique de l'Etat Condensé, CEA-Saclay, F-91191, Gif-sur-Yvette, France
(Received 10 June 1993; revised manuscript received 17 June 1994)

We have measured the current-voltage characteristic of a small capacitance tunnel junction coupled to a transmission line resonator. We calibrate the resonator using the sharp resonances displayed by the junction in the superconducting state, which corresponds to the pumping of the modes of the resonator by the ac Josephson current. With this calibration, we explain quantitatively the nonlinearity of the junction characteristic in the normal state as being due to the process by which a single electron tunnels by emitting a photon, the basic process of the theory of the effect of the electromagnetic environment on tunneling.

PACS numbers: 74.50.+r, 73.40.Gk, 73.40.Rw

In 1986, Averin and Likharev [1] proposed that the discreteness of charge transfer through a metal-insulator-metal tunnel junction, which does not normally manifest itself on its current-voltage characteristic, could be revealed by current biasing a junction with a capacitance C small enough that the charging energy of a single electron $e^2/2C$ would be much larger than the thermal energy k_BT. Several theoretical works [2–5] subsequently showed that this charging effect only takes place if the tunneling of a single electron excites at least one mode of the bias circuit, often referred to as the "electromagnetic environment" of the junction. A well-studied case is when the environment consists of a perfect dc bias current source in parallel with a frequency independent resistor R. Such an environment has a continuous density of modes whose dimensionless coupling strength to the junction is given by R/R_K, where $R_K = h/e^2$. Single-electron charging effects have indeed been observed for a well-controlled resistive environment such that $R/R_K > 1$ [6]. Another case which is particularly simple is when the impedance $Z(\omega)$ of the environment is sharply peaked in frequency [3,5], i.e., $Z(\omega) \simeq [i\pi C_r(\omega - \omega_r - i\eta)]^{-1}$ for $\omega \sim \omega_r \gg \eta$. Unlike a frequency-independent resistor which manifests itself by a smooth nonlinearity in the current-voltage $I(V)$ characteristic of the junction, a resonator is expected to produce a step in the differential conductance $dI(V)/dV$, a feature which is the direct manifestation of elementary events whereby a single electron tunnels by emitting one photon in the resonator. The voltage location and relative magnitude of this step are $V = (\hbar/e)\omega_r$ and $[R_K C_r \omega_r]^{-1}$, where ω_r and C_r^{-1} are the angular frequency and weight of the resonance, respectively. In this Letter we report the results of an experiment in which, for the first time, a small capacitance junction has been placed in an environment with well-characterized resonances, and with which the concept of photon-emitting single-electron tunnel events can be quantitatively tested.

The principle of our experiment is depicted in Fig. 1(a). A small capacitance tunnel junction is biased by a voltage source through a specially designed, on-chip coplanar transmission line approximating a quarter wavelength resonator. The junction is fabricated at the end of the transmission line by the overlap of the central strip and the ground plane [7]. The transmission line consists of two sections with the same length l and propagation velocity v but with different characteristic impedances Z_1 and $Z_2 < Z_1$. Because of this impedance discontinuity, the transmission line resonates in general at frequencies $\omega_n = \pi n v/2l$. The transmission line is terminated at the voltage source end by an impedance $Z_x(\omega)$ which represents the system of leads and which is such that $\mathrm{Re}[Z_x(\omega)] \gg Z_2^2/Z_1$. Under this condition, the real part of the impedance $Z(\omega)$ that characterizes the line at the junction will have the strongest peaks at the odd harmonics ω_{2p+1}.

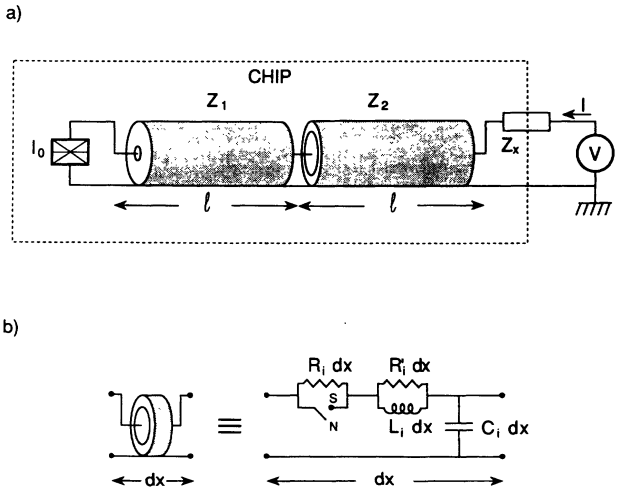

FIG. 1. (a) Schematic of experimental apparatus. The box symbol represents the ultrasmall Josephson junction. (b) Distributed element model of the transmission line. The switch symbolizes the change of model when the line goes from the normal (N) to the superconducting (S) state.

We now demonstrate that the real part of the impedance of the line can be measured *in situ* from the $I(V)$ of the junction in the superconducting state. The theory of the effect of the environment at finite temperature T [5] predicts that when $\mathrm{Re}[Z(\omega_{2p+1})] \ll R_K$ and when $V \gg V_s = \min[ek_BTZ(0)/\hbar, eZ(0)/CR_K]$, the perturbating environment case applicable to our experiment, the current through the superconducting junction is given by

$$I_S = \frac{I_0^2}{2}\frac{Re[Z_t(2eV/\hbar)]}{V} + \mathcal{O}((Z_t/R_K)^2), \qquad (1)$$

where the bias voltage V is assumed to be lower than the gap voltage $2\Delta/e$ and where I_0 denotes the critical current of the junction. The total impedance Z_t seen by the tunneling electrons is given by $Z_t^{-1}(\omega) = Z^{-1}(\omega) + iC\omega$, where C is the junction capacitance. Since our small capacitance junction satisfies $C|Z(\Delta/\hbar)|\Delta/\hbar \ll 1$, $Z_t(\omega)$ almost coincides with $Z(\omega)$ when used in the range of validity of (1). The leading term in Eq. (1) corresponds to the process in which Cooper pair tunneling is correlated with the excitation of one mode of the electromagnetic environment. Interestingly, this term linear in Z_t does not discriminate between the classical or quantum nature of the environment and can be obtained directly from a power balance argument which treats the junction phase difference as a classically diffusing variable and which equates the power IV to the power dissipated in the environment by a sinusoidal current of amplitude I_0 and frequency $2eV/h$ [8]. When $V < V_s$, the environment impedance can no longer be treated perturbatively. The full theory [5] treating multiphoton processes to all order predicts strong deviations from the leading term of Eq. (1) near zero voltage, which have been observed by Kuzmin *et al.* [9] and Haviland *et al.* [10]. These deviations turn the $1/V$ divergence into a peak which, when $Z(0) \ll R_K/4$, is analogous to the supercurrent peak exhibited by the so-called RSJ (resistively shunted junction) model [11].

The theoretical results in the normal state—our main interest—display marked differences with the preceding results for the superconducting state. The perturbative environment theory valid at small voltages [5] predicts a current

$$I_N = \frac{2}{R_K R_N}\int_0^V dV' \int_\epsilon^{V'} \frac{Re[Z_t(eV''/\hbar)]}{V''} dV'' + \mathcal{O}((Z_t/R_K)^2), \qquad (2)$$

where R_N is the tunnel (also called "normal state") resistance of the junction, and where ϵ is a low voltage cutoff such that $I_N/V \to R_N^{-1}$ when $V \to \infty$. The comparison between Eqs. (1) and (2) shows that the coplanar waveguide should manifest itself (i) in the superconducting case as peaks in the $I(V)$ located at $V_{2p+1} \simeq \hbar\omega_{2p+1}/2e$ and whose amplitude involves the product of I_0^2 and the real part of the impedance, and (ii) in the normal case as steps in the first derivative $dI(V)/dV$ located at $2V_{2p+1}$ and whose magnitude involves the ratio of the weight of the resonance to the resistance quantum. Therefore, while the superconducting data should display only the Cooper pair flux quantum $h/2e$, the normal state data should display both the single-electron flux quantum h/e and resistance quantum h/e^2.

Three samples with $l = 1.0$, 1.28, and 1.4 mm were fabricated on oxidized silicon chips using a standard trilayer resist patterned by e-beam lithography, onto which we evaporated two layers of aluminum at two different angles to form simultaneously the junction and the transmission line. The thicknesses of the first and second aluminum layers were 30 and 50 nm, respectively. The two evaporations were separated by an oxidation step to form the tunnel barrier. The junction consisted in fact of two twin junctions in parallel forming a loop with a 17 μm^2 area, which allowed us to vary the Josephson coupling with a magnetic field produced by a small coil placed underneath the sample. The resonating frequency of the loop is high enough that we can characterize this twin junction configuration with only the three parameters I_0, R_N, and C of a single junction. From the 60×60 nm^2 area of the twin junctions, we estimate $C = 1.5 \pm 0.5$ fF. Sections 1 and 2 of the transmission line are characterized by the widths ω_1 and ω_2 of the central strip and the gaps g_1 and g_2 between the central strip and the ground planes. We used the pattern $\omega_1 = 7\ \mu m, \omega_2 = 187\ \mu m, g_1 = 62\ \mu m, g_2 = 14\ \mu m$. From these dimensions and the dielectric constant of silicon $\epsilon_r(\mathrm{Si}) \simeq 12$ [12], we can estimate $Z_1 = 100 \pm 5\,\Omega, Z_2 = 28 \pm 2\,\Omega$, and $v = (1.15 \pm 0.03) \times 10^8$ m/s. The experiments were done with the sample thermally anchored to the mixing chamber of a dilution refrigerator at $T = 22$ mK. All the leads for current and voltage measurements were equipped with filters [13] to prevent noise from reaching the sample. When necessary, the aluminum was driven in the normal state by a 1 T magnetic field.

Figure 2 shows $I(V)$ data of a sample with $l = 1.28$ mm. The large scale data (see inset, curve labeled S) display a sharp current rise corresponding to the superconducting gap $2\Delta/e = 358 \pm 5\,\mu V$. On a finer scale we observe the "supercurrent" peak labeled V_0 accompanied by subgap current peaks whose V-axis positions are labeled V_x, V_y, V_1, V_2, V_3, and V_5. The locations V_{2p+1} and V_2 are in agreement with Eq. (1) if we use a value of v within the error bars of our above estimate. The assignment of the integer numbered peaks to the resonator modes is further confirmed by the other samples with different l whose homologous peaks are located at voltages corresponding to the same value of v. The small bump at V_2 is due to the relatively modest $Z_1/Z_2 \simeq 3.6$ ratio. The two small satellite peaks labeled V_x and V_y are manifestations of a coupling between the transmission line and the ground plane. This interpretation is supported by the fact that, for the other samples, the positions of the V_x and V_y peaks did not scale with l but with the dimensions of the ground plane. The height of all the

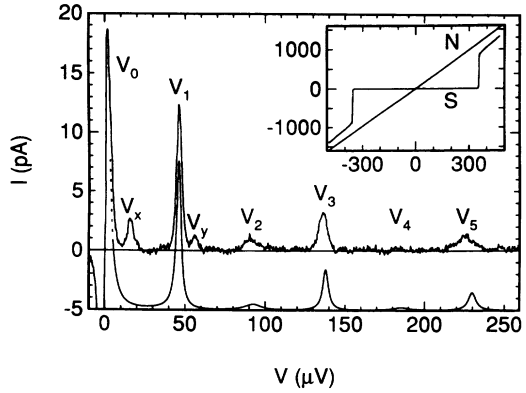

FIG. 2. $I(V)$ data in the superconducting state at 22 mK. The theoretical curve (smooth continuous line), shown with an offset of 5 pA, is a two parameter fit using the transmission line model of Fig. 1. Inset: Large scale $I(V)$ in both normal (N) and superconducting (S) states.

peaks was periodic with respect to the magnetic flux Φ in the junction loop. The modulation curves are well fitted by a $\cos^2(e\Phi/\hbar)$ function (data not shown), which confirms the predicted I_0^2 dependence of the current. The relative modulation depth was 85% for the sample shown and larger than 95% in the other samples. We take this as evidence of adequate junction homogeneity. Note that the resonances of Fig. 2 are similar, but not identical, to the resonances which are observed in the $I(V)$ of a junction, with $E_J \gg E_c$ coupled to a resonator [14], and which involve the nonlinear dynamics of the junction phase difference.

In Fig. 2 we also show in full line the prediction of Eq. (1) with the low temperature Ambegaokar-Baratoff [15] value $I_0 = \pi\Delta/2eR_N = 922 \pm 30$ pA, where $R_N = 305 \pm 10\,\mathrm{k}\Omega$ is the junction resistance in the normal state (see inset of Fig. 2, curve labeled N). To calculate the impedance $Z_t(\omega)$ we have modeled each section of the transmission line by the distributed element model of Fig. 1(b). Each section (indexed by $i = 1, 2$) is characterized by a capacitance per unit length C_i, an inductance per unit length L_i, and the surface losses resistance per unit length R_i'. In the normal case there is one additional parameter, the resistance per unit length R_i. The parameters L_i and C_i are related to the impedance and velocity of the section by $Z_i = \sqrt{L_i/C_i}$ and $v_i = \sqrt{1/L_iC_i}$. For a comparison between the data and the predictions of Eq. (1) using the model of Fig. 1(b) only two fitting parameters are thus needed: the external impedance Z_x, which we take as a pure resistor R_x, and the surface loss resistance R_l', which we take independent of frequency and of section index. At the frequency $\omega_1/2\pi \simeq 22$ GHz, losses were dominated by the contribution from R_x, whereas at higher resonant frequencies $\omega_3/2\pi \simeq 66$ GHz and $\omega_5/2\pi \simeq 110$ GHz, surface losses became important as well. Given $R_x = 110 \pm 10\ \Omega$ from the fitting of $I(V_1)$, we have estimated $R_1' = 50 \pm 30\ \mathrm{k}\Omega/\mathrm{mm}$ from a best fit of $I(V_3)$ and $I(V_5)$. The resulting curve is shown as a solid line in Fig. 2. We did not attempt to fit the supercurrent peak at V_0, since the only available theory for this peak [8] applies when $k_BT \gg E_J$, a condition which was not fulfilled for our data. (In our experiment the Josephson energy $E_J = \hbar I_0/2e$ is much less than E_c.) In summary, apart from the small feature at V_4 which is expected to be lost in the noise, our model for the transmission line correctly reproduces the finite voltage resonances in the experimental $I(V)$. Note that similar resonances have been observed in other experiments on small Josephson junctions [16], but, to our knowledge, they have so far never been quantitatively explained.

In Fig. 3 the comparison between experiment and model shown in Fig. 2 is analyzed in a different form which provides a direct check of the weight of the resonances, an essential information in the comparison between experiment and theory for the normal state junction. We plot, for both the experiment and the transmission line model, the quantity $E(V) = (2e/I_0^2h)\int_0^V UI(U)\,dU$, which has the dimension of the inverse of a capacitance and which would tend towards $(2C)^{-1}$ if, at higher voltages, the breaking of Cooper pairs occurring at $V = 2\Delta/e \simeq E_c/e$ did not interfere with the inelastic Cooper pair tunneling process responsible for the peaks. Apart from a discrepancy in the overall slope which we attribute to a small remaining background current in the experiment due to quasiparticle leakage, there is a good agreement between experiment and theory as far as the height of the steps, i.e., the weight of the resonances, are concerned. It can be shown that, in the limit $Z_1R_x/Z_2^2 \gg 1$, the weight of each odd resonance does not depend on the terminating resistance R_x and to first order, on the surface losses R_l'. We calculate this weight to be given by the value $Z_1v/4l$, shown in Fig. 3 by a vertical bar. There is very good agreement between this value containing no fitted parameters and the experimental values $E(V_2) - E(0)$ and $E(V_4) - E(V_2)$.

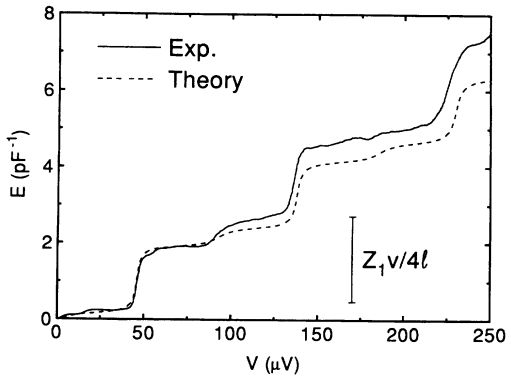

FIG. 3. Plot of the quantity $E(V) = (2e/hI_0^2)\int_0^V UI(U)\,dU$, in which I_0 is obtained, using Ref. [15], from the superconducting gap and the normal state resistance measured from the data in the inset of Fig. 2. The theory curve corresponds to the theory curve of Fig. 2. The calculated step height, which in the limit of sharp resonances is found to depend only on measured parameters, is shown by a vertical bar.

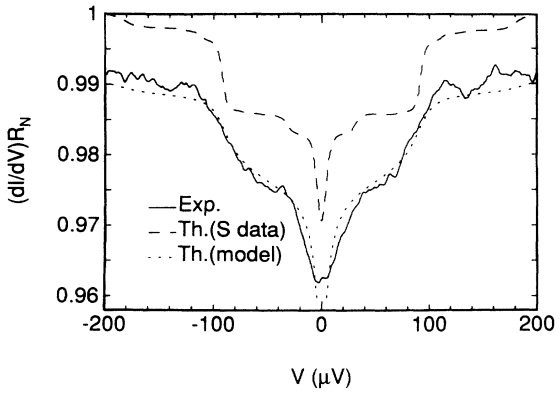

FIG. 4. Derivative of $I(V)$ data, sample brought in the normal state by a 1 T magnetic field, compared with the integral of the $I(V)$ data of Fig. 2, scaled by the theoretical factor $4/R_K I_0^2$ (dashed line). Also shown are predictions of the model of Fig. 1 (dotted line) with the resistance R_t treated as a fit parameter.

In Fig. 4 we plot the results in the normal state in the form $R_N\, dI(V)/dV$. If the environment stayed exactly the same, a comparison between Eqs. (1) and (2) shows that this normalized derivative should be identical, apart from an offset, with the integral quantity $F(V) = 1 - (4/I_0^2 R_K) \int_{V/2}^{V_c} dU\, I(U)$ calculated from the superconducting data (it is convenient to take $2\Delta/e$ for the cutoff voltage V_c). This quantity is plotted in Fig. 4 (dashed line) with a vertical offset allowing a clearer comparison with the normal state data. There is qualitative agreement between the two curves, although the normal state data seem more rounded than the theoretical predictions. We believe this is due to the resistive losses of the transmission line in the normal state. To make a more quantitative comparison we have fitted the normal data with Eq. (2) using the model of Fig. 1(b), with $R_1 = R_2$ treated as a free parameter (the other parameters being the same as in the theoretical curve of Fig. 2). The result of the best fit $R_1 = (2 \pm 1) \times 10^4\ \Omega/\mathrm{m}$ is shown by a dotted line in Fig. 4. This value is consistent with the result $\rho = 8 \times 10^{-9}\ \Omega\,\mathrm{m}$ of a low temperature measurement of the resistivity of an aluminum strip nanofabricated with the same techniques. We see that both the position and magnitude of the V_1 shoulder are well reproduced by theory, the effect of the other resonances being lost in the noise. As expected, the dip at zero voltage is only qualitatively captured.

In conclusion, the $I(V)$ characteristic of a small capacitance Josephson junction coupled to a well-characterized transmission line resonator displays peaks corresponding to Cooper pair tunneling correlated with the excitation of a mode of the resonator. These peaks, whose location and heights calibrate precisely the parameters of the resonator, can also be interpreted as self-induced Shapiro steps [14] in the weak junction–resonator coupling limit. When the junction is brought in the normal state, the derivative of the $I(V)$ shows a step at a voltage located at twice the position of the main peak in the superconducting state. The relative height of the step is given by the ratio of the weight of this main peak, normalized by I_0^2, to the resistance quantum R_K. These results, which agree quantitatively with the theory of the effect of the electromagnetic environment on single-electron tunneling, illustrate the close link between Coulomb blockade and inelastic tunneling.

We would like to thank A. Cleland, H. Grabert, G.-L. Ingold, and K. Likharev for helpful discussions. The technical help of P. F. Orfila is gratefully acknowledged. One of us (T. H.) has benefited from grants from the Otto Mønsted Foundation, the Knud Højgaard Foundation, the Thomas B. Thrige Foundation, the Nato Science Fellowships Programme, and the French Foreign Affair Ministry. This work has been partially supported by the European Community through Contract No. SC1*-CT91-0631.

*Present address: NKT Research Center, Sognevej 11, DK-2605 Brøndby, Denmark.

[1] D. V. Averin and Likharev, J. Low Temp. Phys. **62**, 345 (1986); in *Quantum Effects in Small Disordered Systems*, edited by B. L. Altshuler, P. A. Lee, and R. A. Webb (Elsevier, Amsterdam, 1991).

[2] Yu. V. Nazarov, Pis'ma Zh. Eksp. Teor. Fiz. **49**, 105 (1989) [JETP Lett. **49**, 126 (1989)].

[3] M. H. Devoret, D. Esteve, H. Grabert, G.-L. Ingold, H. Pothier, and C. Urbina, Phys. Rev. Lett. **64**, 1824 (1990).

[4] S. M. Girvin, L. I. Glazman, M. Jonson, D. R. Penn, and M. D. Stiles, Phys. Rev. Lett. **64**, 3183 (1990).

[5] G.-L. Ingold and Yu. V. Nazarov, in *Single Charge Tunneling*, edited by H. Grabert and M. H. Devoret (Plenum, New York, 1992), Chap. 2, and references therein; G.-L. Ingold and H. Grabert, Physica (Amsterdam) **194-196B**, 1025 (1994).

[6] A. N. Cleland, J. M. Schmidt, and J. Clarke, Phys. Rev. Lett. **64**, 1565 (1990).

[7] E. Turlot, D. Esteve, C. Urbina, M. Devoret, S. Linkwitz, and H. Grabert, Phys. Rev. Lett. **62**, 1788 (1989).

[8] See, for instance, K. K. Likharev, *Dynamics of Josephson Junctions and Circuits* (Gordon and Breach, New York, 1986), Chap. 12.

[9] L. S. Kuzmin, Yu. V. Nazarov, D. B. Haviland, P. Delsing, and T. Claeson, Phys. Rev. Lett. **67**, 1161 (1991).

[10] D. B. Haviland, L. S. Kuzmin, P. Delsing, and T. Claeson, Europhys. Lett. **16**, 103 (1991).

[11] A. Barone and G. Paterno, *Physics and Applications of the Josephson Effect* (Wiley, New York, 1982), p. 150.

[12] J. Bethin, T. G. Castner, and N. K. Lee, Solid State Commun. **14**, 1321 (1974).

[13] J. M. Martinis, M H. Devoret, and J. Clarke, Phys. Rev. B **35**, 4682 (1987).

[14] J. Zimmerman, J. Appl. Phys. **42**, 30 (1971).

[15] V. Ambegaokar and A. Baratoff, Phys. Rev. Lett. **10**, 486 (1963); **11**, 104 (1963).

[16] L. J. Geerligs, Ph. D. thesis, Delft University, 1990; L. J. Geerligs, V. F. Anderegg, J. Romijn, and J. E. Mooij, Phys. Rev. Lett. **65**, 377 (1990).

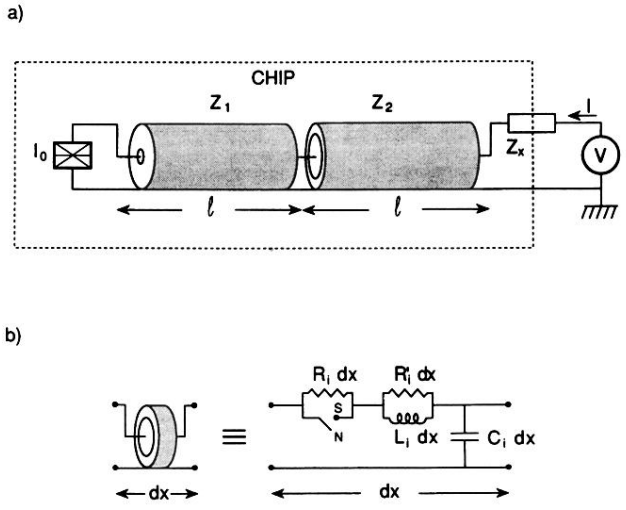

FIG. 1. (a) Schematic of experimental apparatus. The box symbol represents the ultrasmall Josephson junction. (b) Distributed element model of the transmission line. The switch symbolizes the change of model when the line goes from the normal (N) to the superconducting (S) state.